Supplementary Methods

Detection methods used to identify ABL-class cases by DCOG
[Modified from Boer et al., Oncotarget 2017]

Tyrosine kinase fusion detection

Detection of ABL-class tyrosine kinase fusion genes was performed by RT-PCR followed by Sanger sequencing using previously described primers.[1, 2] We used targeted locus amplification for additional cases to detect fusion genes involving *ABL1*, *PDGFRB*, *CSF1R*, and *ABL2* (TLA, Cergentis, Utrecht, the Netherlands).[3, 4] We used break apart FISH with *PDGFRB/CSF1R* and *ABL1* probes (Cytocell) to confirm fusions. The methods applied to each case depended on the type and amount of available patient material.[2]

Genome-wide DNA copy number arrays (array-CGH)

Copy number analysis was performed using Agilent SurePrint G3 Hmn 4x180K arrays (Agilent Technologies, Amstelveen, the Netherlands) co-hybridized with 1 μg patient DNA labeled with ULS-Cy5 and 1 μg reference genomic DNA male pool (G147A, Promega, Leiden, the Netherlands) labeled with ULS-Cy3 (Agilent Genomic DNA ULS Labeling Kit). Copy number microarray data were normalized using median log ratio in the CGHcall [5] version 2.14.0, centralized using CGHnormaliter[6] version 1.8.0, and segmented and called using CGHcall default settings (-1 for loss, 0 for diploid, 1 for gain and 2 for amplification) in R version 2.14.1.

Multiplex ligation-dependent probe amplification

The SALSA P335 ALL-*IKZF1* (a3) and the SALSA P202 Multiplex Ligation-dependent Probe Amplification (MLPA) assays (MRC-Holland) were used to identify or confirm genomic lesions on the following genes: *IKZF1*, *CDKN2A*, *CDKN2B*, *ETV6*, *PAX5*, *RB1*, *BTG1* and *EBF1* as described previously.[7, 8] In short, 125 ng of genomic DNA was used to generate DNA fragments with incorporated FAM nucleotides according to the manufacturer's protocol. The amplified fragments were quantified using an ABI-3130 genetic analyzer (Applied Biosystems, Carlsbad, CA). Peak intensities were normalized to the manufacturer's control probes and to a synthetic control reference generated from five normal DNA samples in the same MLPA run. A peak ratio lower than 0.75 was considered a deletion, a ratio between 0.75 and 1.3 was considered normal copy number, a ratio higher than 1.3 was considered a gain in copy number.

Targeted locus amplification

Targeted Locus Amplification (TLA) combined with deep-sequencing was used to detect fusion genes and sequence mutations in regions up to 100 kb around a pre-selected primer pair by crosslinking of physically proximal genomic sequences as described before.[3] Briefly, DNA and protein in 10-15 million viable leukemic blast cells were crosslinked in a 2% formaldehyde solution. Cells were lysed and DNA was digested with NlaIII, followed by ligation, de-crosslinking and DNA purification. DNA molecules were trimmed with NspI and ligated at a concentration of 5 ng/μl to promote intramolecular ligation to DNA fragments of approximately 2 kb. These chimeric fragments were PCR amplified, sonicated and adaptor-ligated for paired-end high-throughput Illumina sequencing. A total of 31 primer sets targeting 19 recurrently affected genes were designed and multiplexed, including the genes involved in the classical cytogenetic subtypes *MLL*, *RUNX1*, *TCF3*, and *IKZF1*, the tyrosine

kinase genes *ABL1*, *ABL2*, *PDGFRB*, *CSF1R*, *JAK1*, *JAK2*, *JAK3*, *FLT3*, and *TYK2*, and the cytokine signaling genes *CRLF2*, *EPOR*, *IL7R*, *TSLP*, *SH2B3*, and *IL2RB*.[9]

Fluorescent in-situ hybridization (FISH)
FISH was performed on interface nuclei using break apart probes (Cytocell, Cambridge, UK) for *PDGFRB* and *ABL1*. The FISH probes for *PDGFRB* overlap with the neighboring *CSF1R* locus. At least 100 interphase nuclei were evaluated.

Reverse transcriptase PCR (RT-PCR)
cDNA was synthesized from 1 µg total or copy RNA using M-MLV reverse transcriptase and combined oligo-dT and pdN6 priming in 20 µl (Promega, Madison, WI). PCR was performed on 2.5 µl cDNA using Taq polymerase, $MgCl_2$ and buffer from Applied Biosystems (Bleiswijk, Netherlands). For primer sequences see.[2]

References

1. Roberts KG, Morin RD, Zhang J, et al. Genetic alterations activating kinase and cytokine receptor signaling in high-risk acute lymphoblastic leukemia. *Cancer Cell* 2012; **22**(2): 153-66.
2. Boer JM, Steeghs EM, Marchante JR, et al. Tyrosine kinase fusion genes in pediatric BCR-ABL1-like acute lymphoblastic leukemia. *Oncotarget* 2017; **8**(3): 4618-28.
3. de Vree PJ, de Wit E, Yilmaz M, et al. Targeted sequencing by proximity ligation for comprehensive variant detection and local haplotyping. *Nat Biotechnol* 2014; **32**(10): 1019-25.
4. Kuiper RP, Van Reijmersdal SV, Simonis M, et al. Targeted locus amplification & next generation sequencing for the detection of recurrent and novel gene fusions for improved treatment decisions in pediatric acute lymphoblastic leukemia. *Annual Meeting Abstracts Blood* 2015; **126**(23): 696.
5. van de Wiel MA, Kim KI, Vosse SJ, van Wieringen WN, Wilting SM, Ylstra B. CGHcall: calling aberrations for array CGH tumor profiles. *Bioinformatics* 2007; **23**(7): 892-4.
6. van Houte BP, Binsl TW, Hettling H, Pirovano W, Heringa J. CGHnormaliter: an iterative strategy to enhance normalization of array CGH data with imbalanced aberrations. *BMC Genomics* 2009; **10**: 401.
7. Van der Veer A, Waanders E, Pieters R, et al. Independent prognostic value of BCR-ABL1-like signature and IKZF1 deletion, but not high CRLF2 expression, in children with B-cell precursor ALL. *Blood* 2013; **122**(15): 2622-9.
8. Boer JM, Koenders JE, van der Holt B, et al. Expression profiling of adult acute lymphoblastic leukemia identifies a BCR-ABL1-like subgroup characterized by high non-response and relapse rates. *Haematologica* 2015; **100**(7): e261-4.
9. Escherich G, Zur Stadt U, Alawi M, Horstmann M. Rapid capture targeted next generation sequencing (NGS) for detection of genomic kinase- and cytokine receptor rearrangements in B-precursor acute lymphoblastic leukemia. *Annual Meeting Abstracts Blood* 2015; **126**(23): 2609.

Supplementary Tables

Supplementary Table S1: **Overview of ABL-class cases and NCI risk per study group**

Study group	Cases (N)	NCI SR (N)	NCI HR (N)
ANZCHOG	2	0	2
BFM (A, G, CH, Czech, Israel)/AIEOP-family	33	7	26
COALL	8	1	7
COG	25	5	20
DCOG	7	1	6
JACLS/TCCSG/CCLSG	11	2	9
Ma-spore*	7	1	5
UK ALL	29	11	18
Total	122	28	93

* NCI risk of one patient is unknown

Supplementary Table S2: **Partner genes fused 5' of ABL-class genes**

ABL-class type	Fusion Partner	(N)
ABL1 (N=40)	ETV6	7
	FOXP1	2
	NUP214	7
	RANBP2	1
	RCSD1	4
	SNX2	2
	ZMIZ1	16
	Unknown/other	1
ABL2 (N=8)	RCSD1	4
	ZC3HAV1	4
CSF1R (N=10)	MEF2D	2
	SSBP2	8
PDGFRB (N=64)	ATF7IP	4
	CCDC88C	1
	EBF1	50
	ETV6	1
	ZEB2	1
	Unknown/other	7

Supplementary Table S3: **Prognostic value of MRD corrected for NCI risk and treatment arm**

Variable	EFS Hazard Ratio (95%CI)	Cox p-value
Cox univariate model		
MRD EOI $\geq 1 \times 10^{-2}$	3.3 (1.5-7.6)	0.004
Cox multivariate model 1		
MRD EOI $\geq 1 \times 10^{-2}$	3.0 (1.3-6.9)	0.008
NCI high risk	2.2 (0.9-5.3)	0.079
Cox multivariate model 2		
MRD EOI $\geq 1 \times 10^{-2}$	3.7 (1.5-9.0)	0.004
Treatment arm HR	0.7 (0.3-1.6)	0.47

Supplementary Figures

(A)
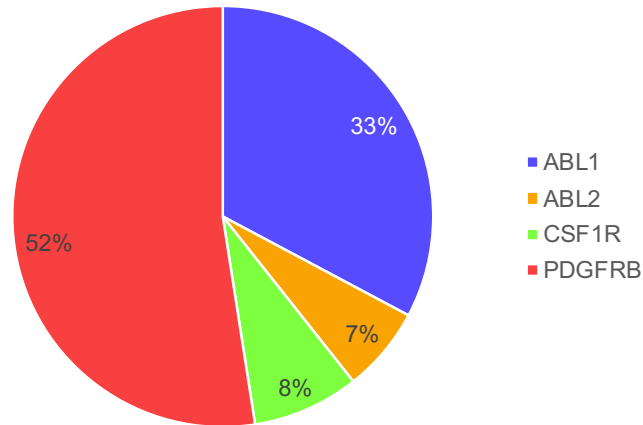
(B)
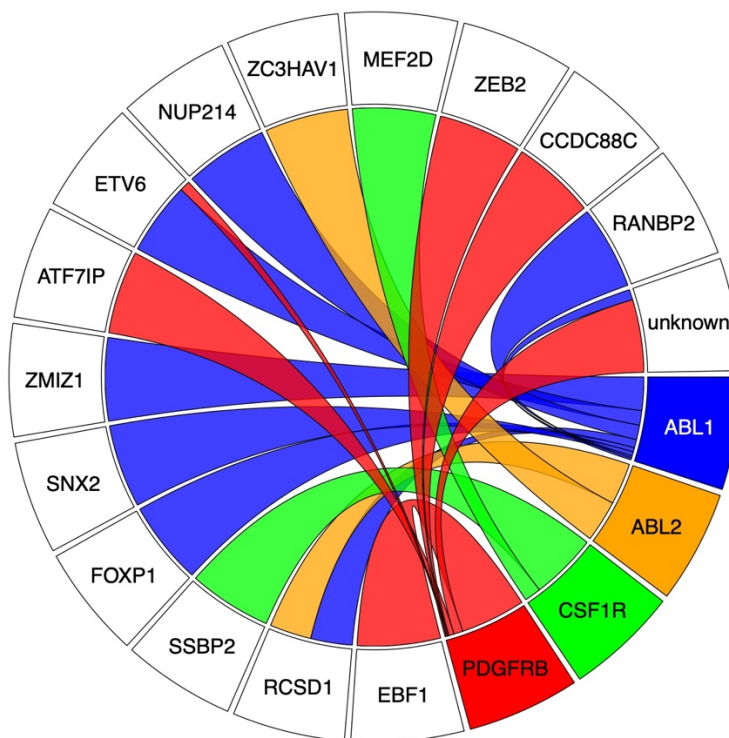
Supplementary Figure S1: **Distribution of ABL-class fusion genes in children with B-ALL**
(A) Frequency of the four main ABL-class types detected in 122 newly diagnosed children with B-ALL.
(B) Circos plot of partner genes fused to *ABL1* (blue), *ABL2* (orange), *CSF1R* (green) and *PDGFRB* (red).
Each partner gene is set to 100% and illustrates to which ABL-class gene the partner genes are most
abundantly fused. E.g. *EBF1* is exclusively fused to *PDGFRB*. Starting from the viewpoint of the ABL-
class gene, one can determine the frequency of partner genes to which the ABL-class gene is fused;
e.g. *PDGFRB* can be fused to at least 5 partner genes (*EBF1, ATF7IP, ETV6, ZEB2, CCDC88C*), with
EBF1-PDGFRB being the most prominent fusion partner.

(A) Age at diagnosis
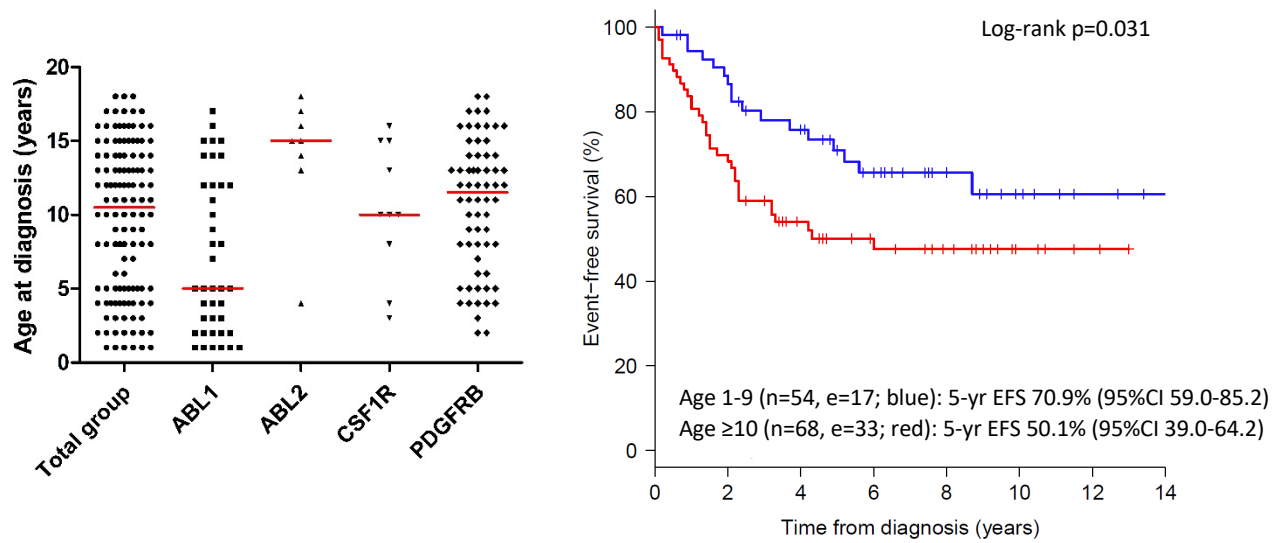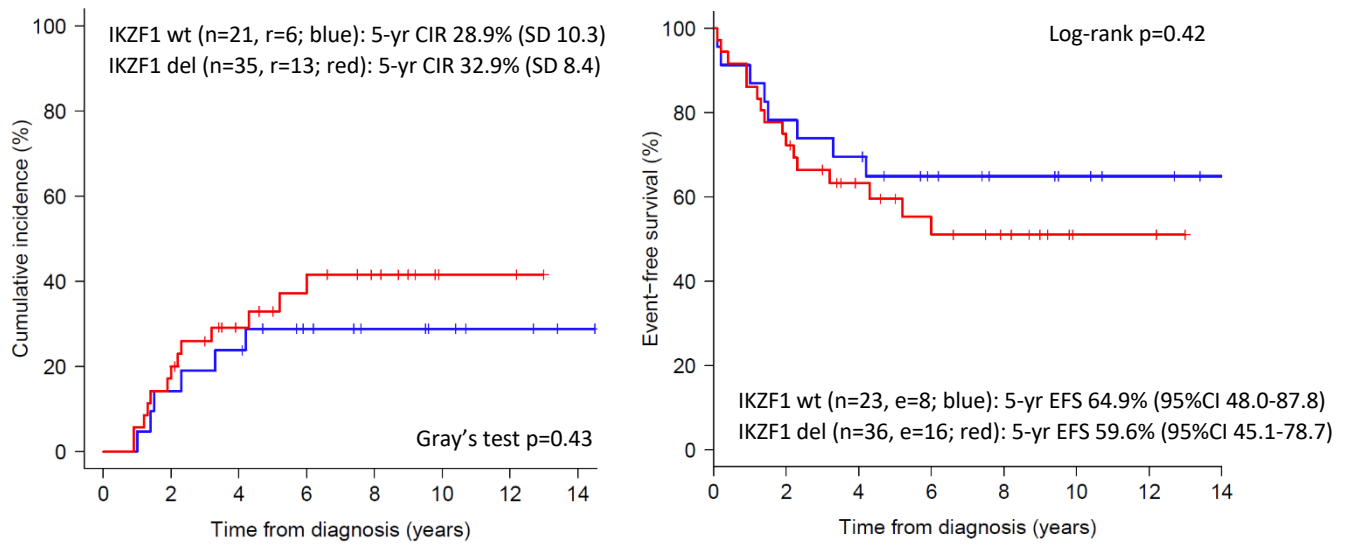

(B) White blood cell count at diagnosis
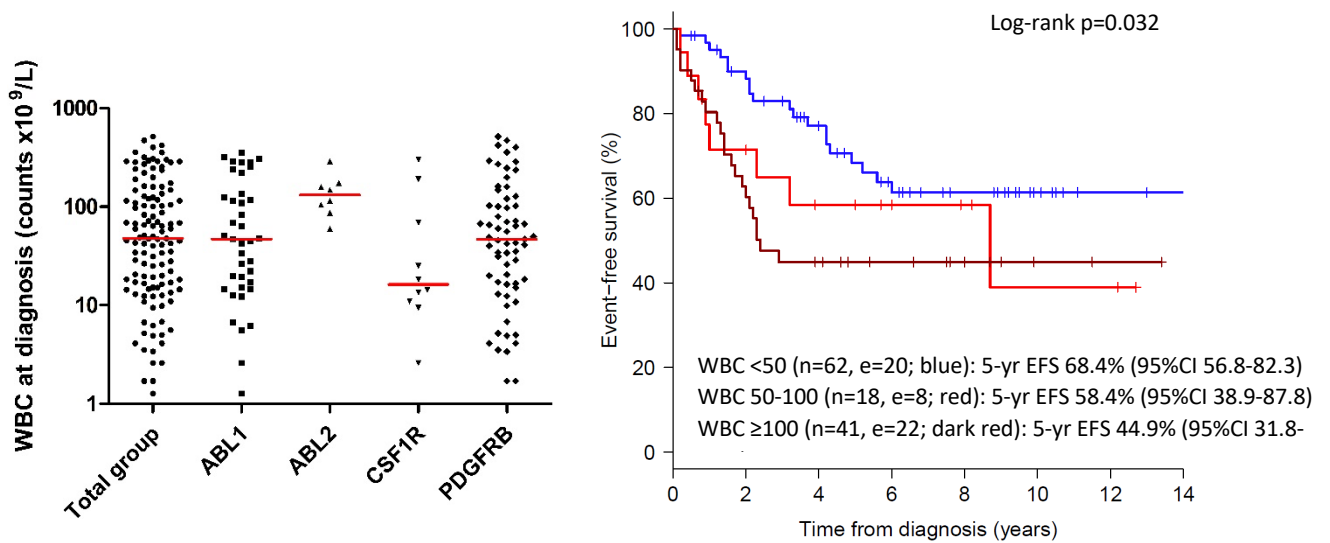
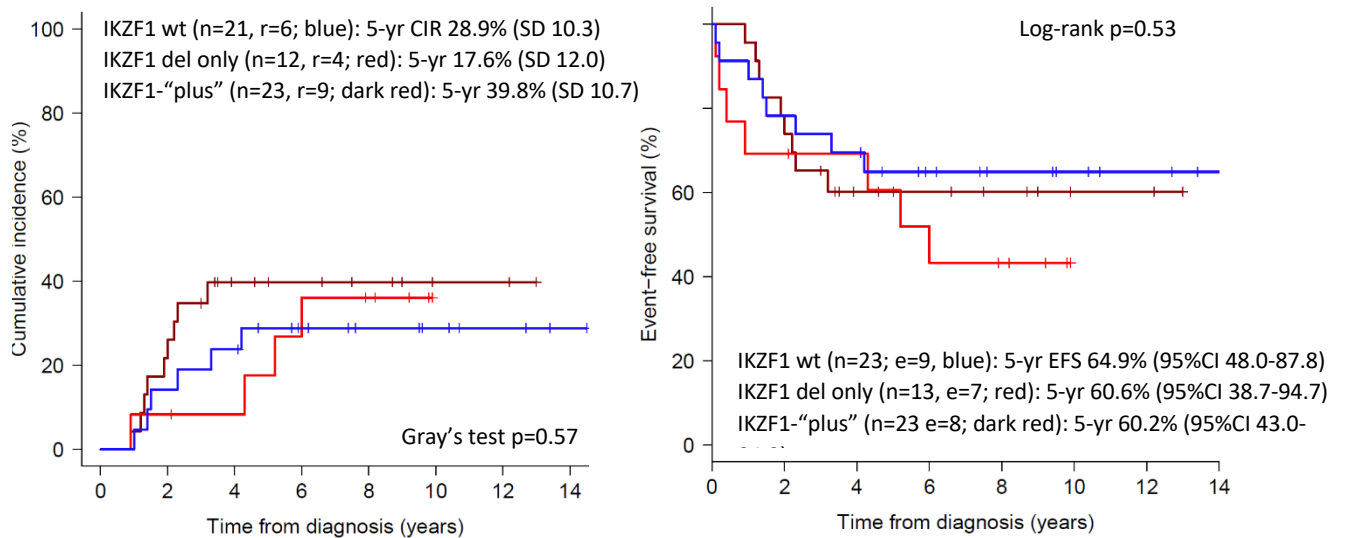***Supplementary Figure S2:*** **Age and white blood cell count (WBC) at diagnosis in ABL-class patients**
(A) Left panel: age distribution across four types of ABL-class, red line indicates median. Age was registered in years as discrete value. Kruskal-Wallis p=0.00028. *ABL2* versus *ABL1*, p=0.00022 and P*DGFRB* versus *ABL1*, p=0.00084. Right panel: 5-year EFS by age categories 1-9 years (n=54, e=17; blue) 70.9% (95%CI 59.0-85.2) and 10-18 years (n=68, e=33; red) 50.1% (95%CI 39.0-64.2; log-rank p=0.031).
(B) Left panel: distribution of WBC across four types of ABL-class, red line indicates median. Right panel: 5-year EFS by WBC categories <50 x10^9/L (n=62, e=20; blue) 68.4% (95%CI 56.8-82.3), 50-100 x10^9/L (n=18, e=8; red) 58.4% (95%CI 38.9-87.8), and ≥100 x10^9/L (n=41, e=22; dark red) 44.9% (95%CI 31.8-63.4; log-rank p=0.032). WBC<50 x10^9/L versus WBC≥50 x10^9/L, log-rank p=0.012;

(A) Clinical outcome of ABL-class patients harboring an *IKZF1* deletion

IKZF1 wt (n=21, r=6; blue): 5-yr CIR 28.9% (SD 10.3)
IKZF1 del (n=35, r=13; red): 5-yr CIR 32.9% (SD 8.4)

Gray's test p=0.43

Log-rank p=0.42

IKZF1 wt (n=23, e=8; blue): 5-yr EFS 64.9% (95%CI 48.0-87.8)
IKZF1 del (n=36, e=16; red): 5-yr EFS 59.6% (95%CI 45.1-78.7)

(B) Clinical outcome of ABL-class patients harboring an *IKZF1* deletion with and without lesions in *PAX5/CDKN2A/2B*

IKZF1 wt (n=21, r=6; blue): 5-yr CIR 28.9% (SD 10.3)
IKZF1 del only (n=12, r=4; red): 5-yr 17.6% (SD 12.0)
IKZF1-"plus" (n=23, r=9; dark red): 5-yr 39.8% (SD 10.7)

Gray's test p=0.57

Log-rank p=0.53

IKZF1 wt (n=23; e=9, blue): 5-yr EFS 64.9% (95%CI 48.0-87.8)
IKZF1 del only (n=13, e=7; red): 5-yr 60.6% (95%CI 38.7-94.7)
IKZF1-"plus" (n=23 e=8; dark red): 5-yr 60.2% (95%CI 43.0-

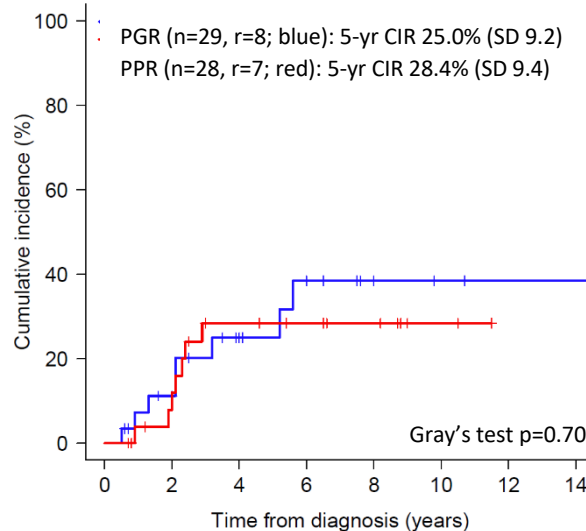*Supplementary Figure S3:* **Prognostic value of *IKZF1* deletion w/wo deletions in *PAX5*, *CDKN2A/2B***
(A) CIR (left panel) and EFS (right panel) curves of *IKZF1* wildtype (wt; blue) and *IKZF1*-deleted cases (red). 5-year CIR for 21 *IKZF1* wt 28.9% (SD 10.3) and 35 *IKZF1* del 32.9% (SD 8.4; Gray's test p=0.43). 5-year EFS for 23 *IKZF1* wt 64.9% (95%CI 48.0-87.8) and 36 *IKZF1* del 59.6% (95%CI 45.1-78.7; log-rank p=0.42).
(B) CIR (left panel) and EFS (right panel) curves of *IKZF1* wt (blue), *IKZF1*-deleted cases without (*IKZF1* del only; red) and with (*IKZF1*-"plus", dark red) deletions in *PAX5* and/or *CDKN2A/2B*. 5-year CIR for 21 *IKZF1* wt 28.9% (SD 10.3), 12 *IKZF1* del only 17.6% (SD 12.0) and 23 *IKZF1* "plus" 39.8% (SD 10.7), Gray's p=0.57. 5-year EFS for 23 *IKZF1* wt 64.9% (95%CI 48.0-87.8), for 13 *IKZF1* del only 60.6% (95%CI 38.7-94.7) and for 23 *IKZF1*-"plus" 60.2% (95%CI 43.0-84.3); log-rank p=0.53.

(A)

PGR (n=29, e=10; blue): 5-yr EFS 67.3% (95%CI 50.8-89.1)
PPR (n=28, e=14; red): 5-yr EFS 50.5% (95%CI 34.4-74.0)

(B)

PGR (n=29, r=8; blue): 5-yr CIR 25.0% (SD 9.2)
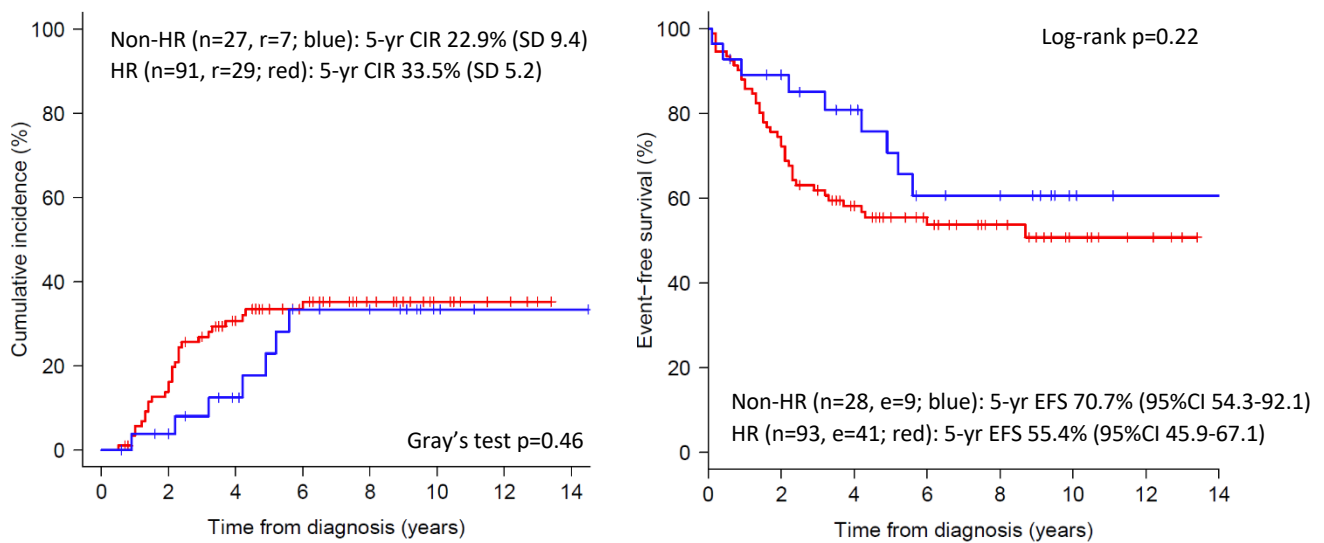PPR (n=28, r=7; red): 5-yr CIR 28.4% (SD 9.4)
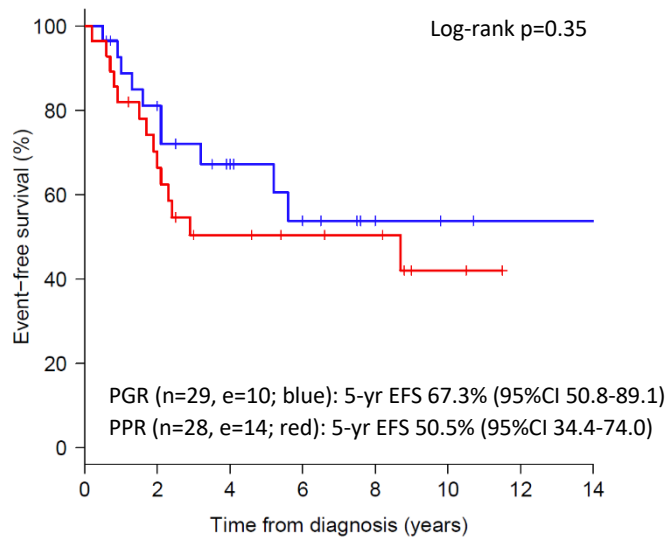
Supplementary Figure S4: **Prognostic value of the prednisone window response in ABL-class patients** A good window response was defined by <1,000 blasts per µl of peripheral blood at day 8 of the therapeutic window, just before start of induction therapy. A good response (PGR) was detected in 29 out of 57 (51%) documented cases (blue line). A poor response (PPR) was defined by ≥1,000 blasts per µl, and was reported in 28 patients (49%), red line.
(A) EFS curve of patients with documented prednisone window response. 5-year EFS for good responders 67.3% (95%CI 50.8-89.1) and for poor responders 50.5% (95%CI 34.4-74.0), log-rank p=0.35. PPR versus PGR HR 1.46 (95% CI 0.65-3.29; Cox p=0.36.
(B) CIR curve of patients with documented prednisone window response. 5-year CIR for good responders 25.0% (SD 9.2) and for poor responders 28.4% (SD 9.4), Gray's test p=0.70.

**(A)** Clinical outcome according to risk-stratification of total group of ABL-class B-ALL cases

Non-HR (n=27, r=7; blue): 5-yr CIR 22.9% (SD 9.4)
HR (n=91, r=29; red): 5-yr CIR 33.5% (SD 5.2)

Gray's test p=0.46

Log-rank p=0.22

Non-HR (n=28, e=9; blue): 5-yr EFS 70.7% (95%CI 54.3-92.1)
HR (n=93, e=41; red): 5-yr EFS 55.4% (95%CI 45.9-67.1)

(B) Clinical outcome according to risk-stratification for *PDGFRB* fusion positive cases only

Non-HR (n=6, r=4; blue): 5-yr CIR 50.0% (SD 23.9)
HR (n=56, r=16; red): 5-yr CIR 31.9% (SD 6.7)

Gray's test p=0.13

Non-HR (n=7, e=6; blue): 5-yr EFS 28.6% (95%CI 8.9-92.2)
HR (n=57, e=24; red): 5-yr EFS 56.5% (95%CI 44.5-71.8)

Log-rank p=0.032
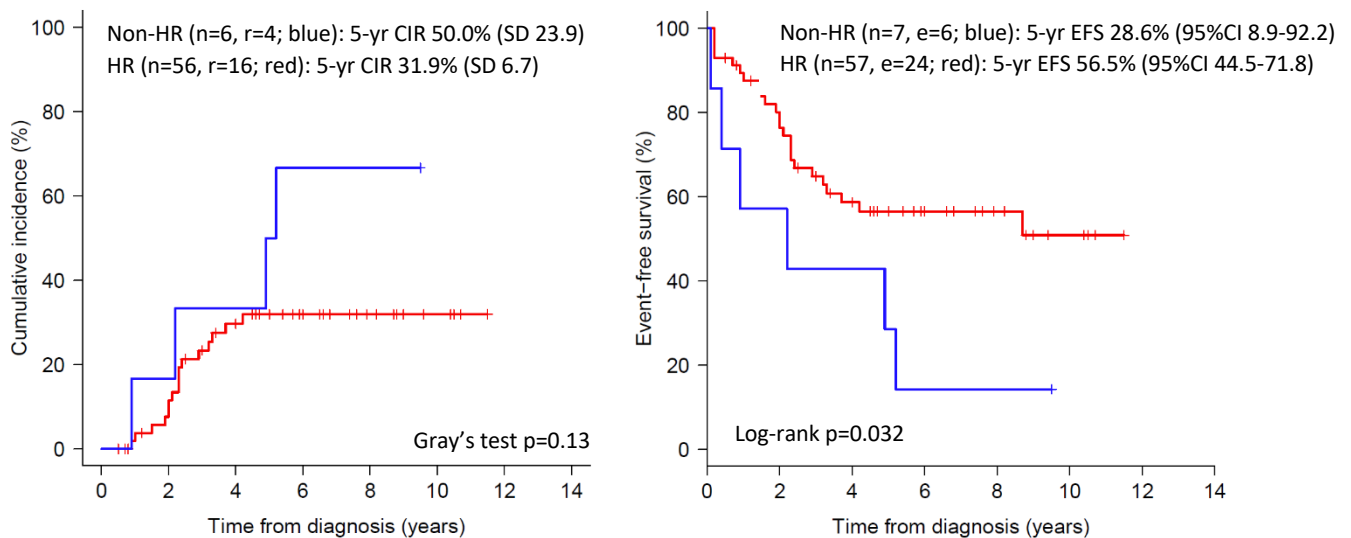
Supplementary Figure S5: **Clinical outcome of ABL-class cases according to the intention to treat (A)** Total group of ABL-class cases. 5-year CIR of non-HR 22.9% (SD 9.4) and 33.5% (SD 5.2) for HR-treated cases. Gray's test p=0.46. 5-year EFS of non-HR 70.7% (95%CI 54.3-92.1) and 55.4% (95%CI 45.9-67.1) for HR-treated cases. Log-rank p=0.22.
(B) *PDGFRB*-fusion cases only. 5-year CIR of non-HR 50.0% (SD 23.9) and 31.9% (SD 6.7) for HR-treated cases. Gray's test p=0.13. 5-year EFS of non-HR 28.6% (95%CI 8.9-92.2) and 56.5% (95%CI 44.5-71.8) for HR-treated cases. Log-rank p=0.032. Hazard ratio for non-HR versus HR 2.57 (95% CI 1.05-6.30), Cox p=0.039.
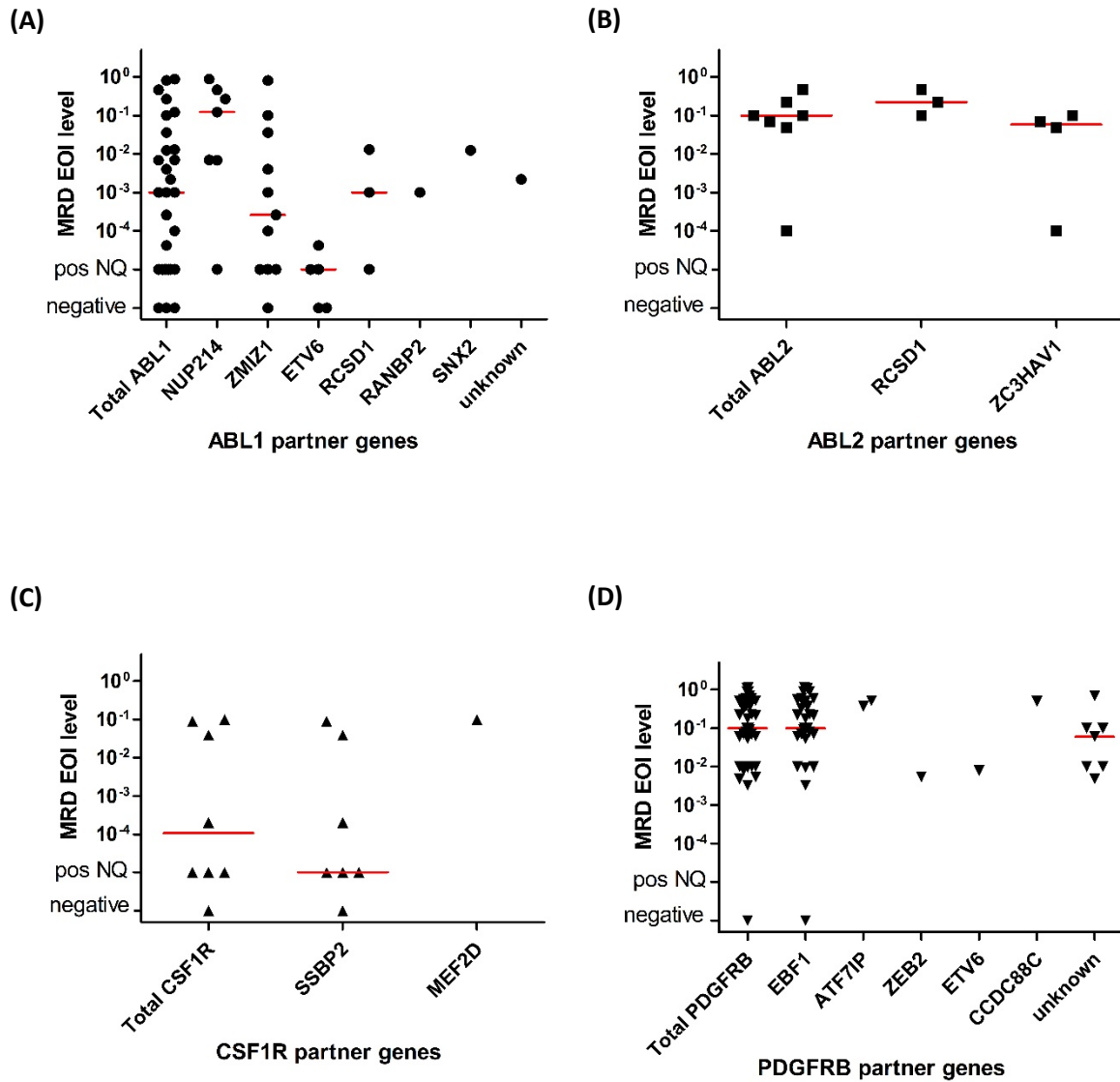
Supplementary Figure S6: **MRD levels for ABL-class fusion genes** Absolute MRD levels at the end of induction (MRD EOI) per ABL-class fusion type and their 5' partner genes. **(A)** *ABL1*, **(B)** *ABL2*, **(C)** *CSF1R* and **(D)** *PDGFRB* fusion cases. Red line represents the median MRD EOI level in each group. Pos NQ, positive but not quantifiable MRD level. Quantitative range for MRD detection was 10^{-4}.
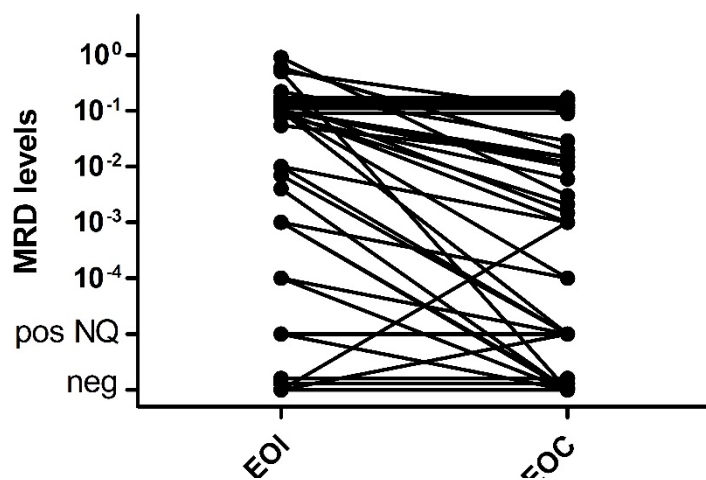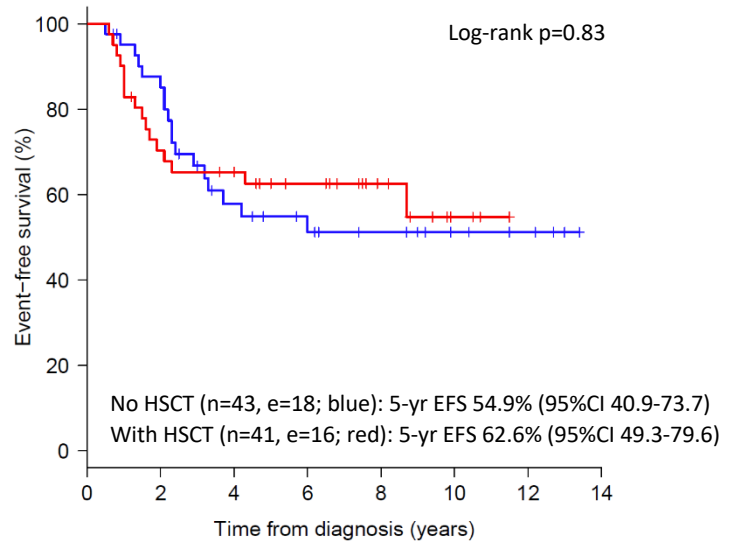
Supplementary Figure S7: **Kinetics of MRD levels in ABL-class patients** Paired analysis of end of induction (EOI) and end of consolidation (EOC) MRD levels in 41 ABL-class patients. Seven (17%) of these patients had negative or positive but not quantifiable MRD levels (i.e. below $<10^{-4}$) at EOI which increased towards 16 (39%) at EOC. Wilcoxon matched pairs test, p<0.0001.

(A)
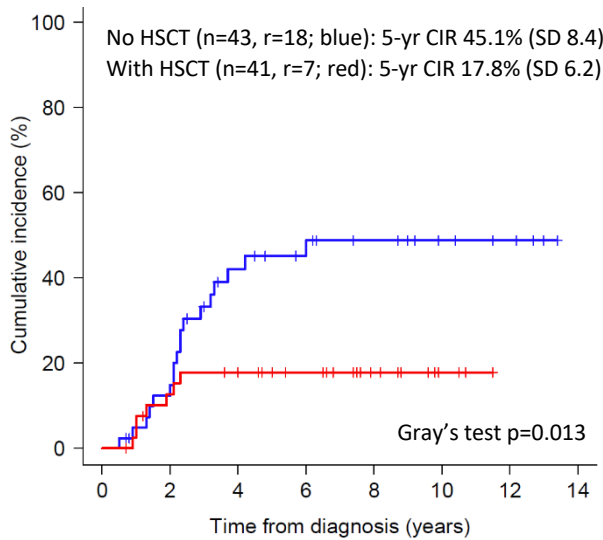
(B)

(C)
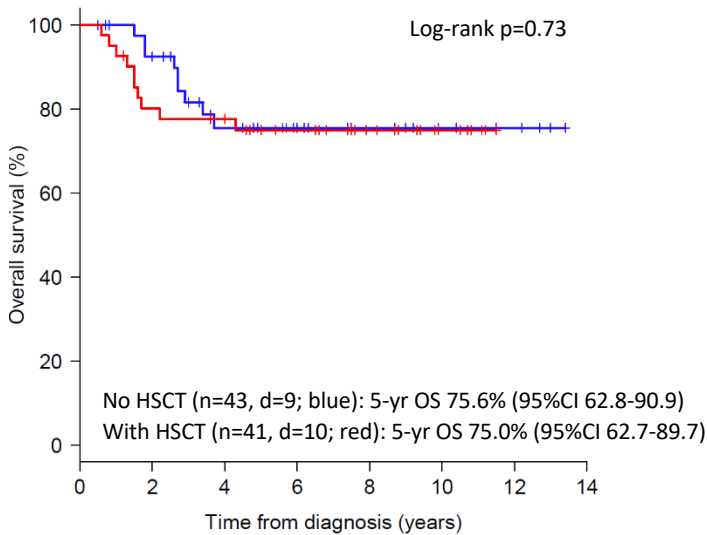
Supplementary Figure S8: **Effect of hematopoietic stem cell transplantation on outcome of HR-treated ABL-class patients** Outcome of HR-treated patients with and without hematopoietic stem cell transplantation (HSCT) given at first complete remission. Only HR-treated patients without an event in the first 6 months from diagnosis were included to (landmark analysis).

(A) CIR for HR-treated patients with (n=41, r=7; red) and without (n=43, r=18; blue) HSCT. Gray's test p=0.013.

(B) EFS for HR-treated patient who did (n=41, e=16; red) or did not (n=43, e=18; blue) receive an HSCT. Log-rank p=0.83.

(C) OS for HR-treated patient who did (n=41, d=10; red) or did not (n=43, d=9; blue) receive an HSCT. Log-rank p=0.73.

Patients' features | **ABL class** | **ABL1** | **ABL2** | **CSF1R** | **PDGFRB** | **Refs #**

Patients' features	ABL class	ABL1	ABL2	CSF1R	PDGFRB	Refs #
age/WBC						
Pred window response						[1] (ABL class);
% IKZF1 deletion						this study (ABL class and subtype)
MRD levels						
EFS/%events						

Response to TKI

Response to TKI	ABL class	ABL1	ABL2	CSF1R	PDGFRB	
in vitro (Ba/F3, Arf-/-)						[2-6]
ex vivo (patients' cells)			?			[5, 7]
in vivo mouse model						[2, 3, 5, 8]
pediatric patients				?		[3, 9-17] (case studies)
						[1, 18] (small sized groups)

Color legend:

Patients' features:

- extreme unfavorable
- very unfavorable
- unfavorable
- favorable

Response to TKI:

- highly sensitive to TKI
- moderate sensitive to TKI

Supplementary Figure S9: **Overview of compiled evidence** Clinical and prognostic features of ABL-class patients as group and per ABL-class fusion type (upper panel, excluding descriptive studies) and preclinical and patients' response data (case studies and small sized pilot studies) obtained about the sensitivity of ABL-class fusion genes to TKIs. *Ex vivo* studies comprise TKI efficacy assays using primary leukemic cells of patients or patient-derived xenograft cells. Question mark indicates absence of relevant data.

References of Figure S9:

1. Cario, G., et al., *Relapses and treatment-related events contributed equally to poor prognosis in children with ABL-class fusion positive B-cell acute lymphoblastic leukemia treated according to AIEOP-BFM protocols.* Haematologica, 2019.
2. Roberts, K.G., et al., *Genetic alterations activating kinase and cytokine receptor signaling in high-risk acute lymphoblastic leukemia.* Cancer Cell, 2012. **22**(2): p. 153-66.
3. Roberts, K.G., et al., *Targetable kinase-activating lesions in Ph-like acute lymphoblastic leukemia.* N Engl J Med, 2014. **371**(11): p. 1005-15.
4. Tomita, O., et al., *Sensitivity of SNX2-ABL1 toward tyrosine kinase inhibitors distinct from that of BCR-ABL1.* Leuk Res, 2014. **38**(3): p. 361-70.

5. Roberts, K.G., et al., *Oncogenic role and therapeutic targeting of ABL-class and JAK-STAT activating kinase alterations in Ph-like ALL.* Blood Adv, 2017. **1**(20): p. 1657-1671.
6. Ishibashi, T., et al., *Ph-like ALL-related novel fusion kinase ATF7IP-PDGFRB exhibits high sensitivity to tyrosine kinase inhibitors in murine cells.* Exp Hematol, 2016. **44**(3): p. 177-88 e5.
7. Lilljebjorn, H., et al., *RNA-seq identifies clinically relevant fusion genes in leukemia including a novel MEF2D/CSF1R fusion responsive to imatinib.* Leukemia, 2014. **28**(4): p. 977-9.
8. Tasian, S.K., et al., *Potent efficacy of combined PI3K/mTOR and JAK or ABL inhibition in murine xenograft models of Ph-like acute lymphoblastic leukemia.* Blood, 2017. **129**(2): p. 177-187.
9. Lengline, E., et al., *Successful tyrosine kinase inhibitor therapy in a refractory B-cell precursor acute lymphoblastic leukemia with EBF1-PDGFRB fusion.* Haematologica, 2013. **98**(11): p. e146-8.
10. Weston, B.W., et al., *Tyrosine kinase inhibitor therapy induces remission in a patient with refractory EBF1-PDGFRB-positive acute lymphoblastic leukemia.* J Clin Oncol, 2013. **31**(25): p. e413-6.
11. Kobayashi, K., et al., *TKI dasatinib monotherapy for a patient with Ph-like ALL bearing ATF7IP/PDGFRB translocation.* Pediatr Blood Cancer, 2015. **62**(6): p. 1058-60.
12. Perwein, T., et al., *Imatinib-induced long-term remission in a relapsed RCSD1-ABL1-positive acute lymphoblastic leukemia.* Haematologica, 2016. **101**(8): p. e332-5.
13. Schwab, C., et al., *EBF1-PDGFRB fusion in pediatric B-cell precursor acute lymphoblastic leukemia (BCP-ALL): genetic profile and clinical implications.* Blood, 2016. **127**(18): p. 2214-8.
14. Fazio, F., et al., *Efficacy of imatinib and chemotherapy in a pediatric patient with Philadelphia-like acute lymphoblastic leukemia with Ebf1-Pdgfrb fusion transcript.* Leuk Lymphoma, 2020. **61**(2): p. 469-472.
15. Decool, G., et al., *Efficacy of Tyrosine Kinase Inhibitor Therapy in a Chemotherapy-refractory B-cell Precursor Acute Lymphoblastic Leukemia With ZC3HAV1-ABL2 Fusion.* Hemasphere, 2019. **3**(3): p. e193.
16. Sakurai, Y., et al., *B-Cell Precursor-Acute Lymphoblastic Leukemia With EBF1-PDGFRB Fusion Treated With Hematopoietic Stem Cell Transplantation and Imatinib: A Case Report and Literature Review.* J Pediatr Hematol Oncol, 2020.
17. Zaliova, M., et al., *Characterization of leukemias with ETV6-ABL1 fusion.* Haematologica, 2016. **101**(9): p. 1082-93.
18. Tanasi, I., et al., *Efficacy of tyrosine kinase inhibitors in Ph-like acute lymphoblastic leukemia harboring ABL-class rearrangements.* Blood, 2019. **134**(16): p. 1351-1355.